# The Disturbance Reduction System: Testing Technology for Drag-Free Operation

John Hanson[a*], G. Mac Keiser[b], Saps Buchman[b], Robert Byer[b], Dave Lauben[b], Ben Shelef[c], Gad Shelef[c], Vlad Hruby[d], Manuel Gamero-Castano[d]

[a]CrossTrac Engineering; [b]Hansen Experimental Physics Laboratory, Stanford University; [c]Gizmonics, Inc.; [d]Busek Co., Inc.

## ABSTRACT

The Disturbance Reduction System (DRS) is designed to demonstrate technology required for future gravity missions, including the planned LISA gravitational-wave observatory, and for precision formation-flying missions. The DRS is based on a freely floating test mass contained within a spacecraft that shields the test mass from external forces. The spacecraft position will be continuously adjusted to stay centered about the test mass, essentially flying in formation with the test mass. Any departure of the test mass from a gravitational trajectory is characterized as acceleration noise, resulting from unwanted forces acting on the test mass. The DRS goal is to demonstrate a level of acceleration noise more than four orders of magnitude lower than previously demonstrated in space. The DRS will consist of an instrument package and a set of microthrusters which will be attached to a suitable spacecraft. The instrument package will include two Gravitational Reference Sensors comprised of a test mass within a reference housing. The position of the test mass will be measured with respect to the reference housing by monitoring changes in capacitance between the electrodes on the reference housing, using the test mass as a virtual ground plane. The spacecraft position will be adjusted using colloidal microthrusters, which are miniature ion engines that provide continuous thrust with a range of 1-20 μN with resolution of 0.1 μN. The DRS will be launched in 2007 as part of the ESA SMART-2 spacecraft. The DRS is a project within NASA's New Millennium Program.

Keywords: Disturbance Reduction, Drag Free Satellite, Interferometer, Accelerometer

## 1. INTRODUCTION

Several missions proposed for near term implementation require the development of a new generation of Gravitational Reference Sensor, thrusters capable of providing continuous thrust at the μN level, precision formation flying techniques and the drag-free control laws necessary to tie them all together. Missions requiring drag free sensing and control improvements include the Laser Interferometer Space Antenna (LISA, which will search for low frequency gravitational waves), EX-5 (mapping of time varying Earth gravitational fields) and LIRE (test of General Relativity). These missions require improvements to existing gravitational sensors of several orders of magnitude in both residual acceleration and low frequency coverage. The technology demonstrated by DRS will support several anticipated formation flying interferometer missions as well, including TPF (infrared imaging of planetary systems), MAXIM (x-ray interferometry) and Stellar Imager (UV imaging of star systems).

The gravitational reference sensor (GRS) is central to the operation of a drag free satellite. First flown in 1973 as TRIAD-1[1], the goal of drag free satellites is to fly a perfectly gravitational trajectory. This is achieved by building a spacecraft around a test mass, sensing the position of the test mass relative to the spacecraft and firing thrusters to control the position of the spacecraft such that the test mass "floats" inside its housing, unaffected by the spacecraft or external disturbances. Because the spacecraft is following the trajectory of the undisturbed test mass, it is also flying a drag-free trajectory. Alternately, the test mass can be forced to follow the trajectory of the spacecraft, at which point the GRS becomes an accelerometer and the force required to keep it centered in its housing is a measure of the acceleration of the spacecraft. In either case, the key performance metric for a gravitational reference sensor is the *residual specific force* in the frequency band of interest. These extraneous forces come from several sources, including mass attraction between the test mass and the spacecraft, residual gas pressure in the housing, interactions between the proof mass and magnetic fields and forces used to constrain the test mass in non-sensitive degrees of freedom.

* hanson@netwizards.net; phone 1 650 255-0168; CrossTrac Engineering, 437 Costa Mesa Terrace, Unit G, Sunnyvale, CA, 94087

The Disturbance Reduction System mission has two key objectives: to demonstrate the operation of a gravitational reference sensor with residual specific force levels in the sensitive axis at or below $3 \cdot 10^{-14}$ m/(s$^2 \cdot \sqrt{\text{Hz}}$) between 1 mHz and 10 mHz; and to demonstrate a system for sensing the position of the proof mass relative to the housing with an accuracy of $3 \cdot 10^{-9}$ m/$\sqrt{\text{Hz}}$. A measurement of the specific force of a GRS cannot be performed on the earth to this level of precision. Recent experiments at Trento have demonstrated the ability to measure residual specific force in a GRS at the $6 \cdot 10^{-12}$ m/(s$^2 \cdot \sqrt{\text{Hz}}$) level, but only in a narrow frequency band around 0.24 Hz [2]. The only way to demonstrate the performance of the GRS at the required levels is to perform an experiment in space and away from the Earth's gravity field. DRS, in conjunction with its sister test package, LISA Test Package (LTP), will fly on the SMART-2 spacecraft in 2006 to demonstrate this technology.

The GRS being developed for this mission consists of an Au/Pt cube 4 cm on a side, a ceramic housing with gold plated electrodes, a titanium vacuum can to constrain the ceramic plates, a pneumatic caging mechanism, a UV charge control system and associated electronics. Sensing of the proof mass position within its housing is done capacitively with a set of 14 electrodes. These same electrodes exert the electrostatic forces for the constraint of necessary degrees of freedom, primarily being the rotation of the proof mass and translation in the non-sensitive degrees of freedom.

As shown in Figure 1, the residual specific force acting on the GRS will be measured by flying two GRS's on the same spacecraft. The positions of the two test masses will be measured relative to one another in the sensitive direction with an interferometer. The positions of the two test masses relative to their housings are sensed capacitively and a set of eight colloidal microthrusters provided by Busek Co. are used to fly the spacecraft about the primary test mass. By properly controlling the spacecraft rotation degrees of freedom, the second test mass can be unconstrained in its two transverse degrees of freedom as well. However, the sensitive axis of the secondary test mass will not be drag free. Low frequency forces (below the measurement band), the result of spacecraft mass attraction, and electrostatic and magnetostatic fields, will cause the secondary test mass to drift in the sensitive direction if it is not constrained. On DRS, the motion of the secondary test mass is controlled below 1 mHz by forcing the test mass electrostatically.

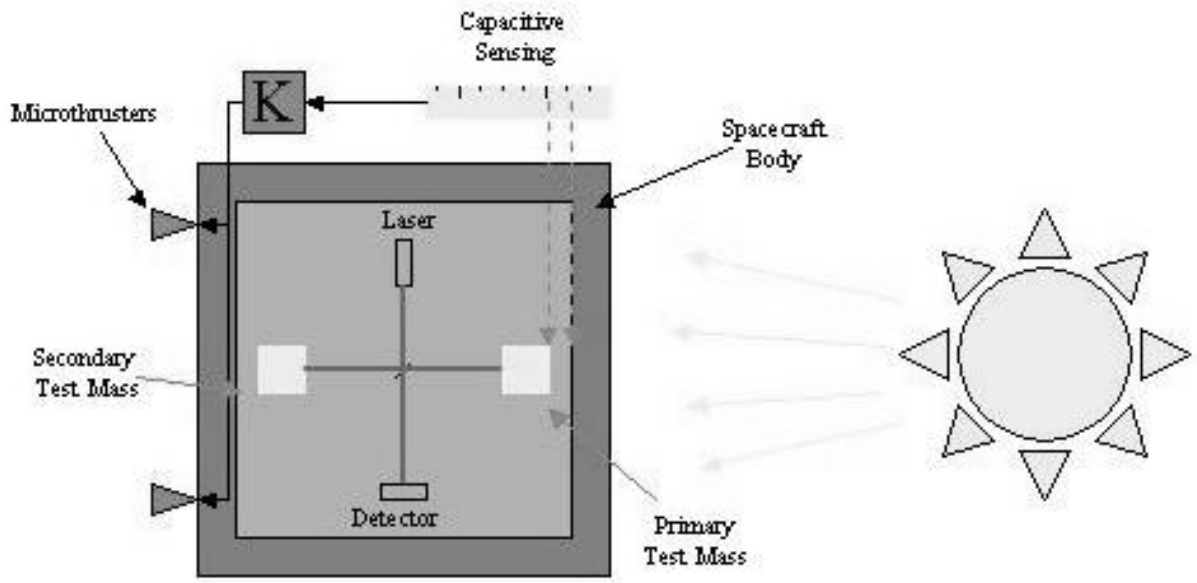


Figure 1: DRS Mission Concept

## 2. GRAVITATIONAL REFERENCE SENSOR

The core of the GRS (Figure 2) is a 4 cm cube made of a 73% gold and 27% platinum alloy selected specifically for its low magnetic susceptibility (measurements have been made verifying that it is less than $5 \cdot 10^{-6}$). The test mass is positioned at the center of a beryllia housing with 2 mm gaps on all sides. The housing is constructed from six plates, each with gold sputtered electrodes and ground planes. The innovative electrode configuration permits the sensing and control of all three rotation degrees of freedom and the two transverse (non-sensitive) degrees of freedom without using electrodes in the sensitive direction. Two additional electrodes provide a measurement of the proof mass position in the sensitive direction. These can used to force the test mass in the sensitive direction when necessary.

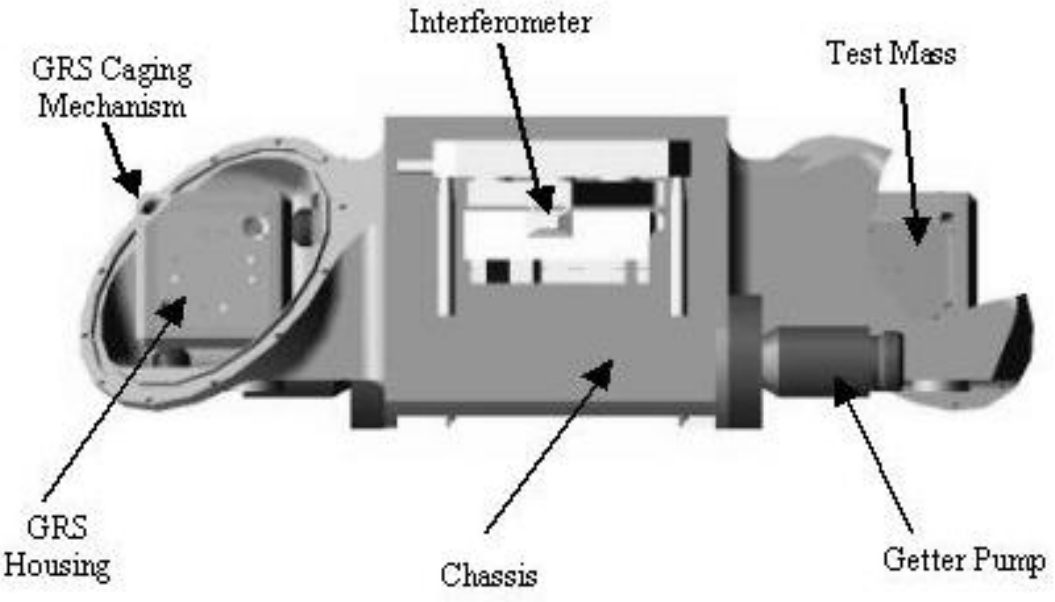


Figure 2: GRS, Chassis and Interferometer

The housing electrodes are connected to the sensing and forcing electronics, shown in Figure 3. While it is based on the GP-B (Gravity Probe B) electrostatic suspension system[3], it represents a significant improvement over the voltage drive used there. A voltage drive controls the voltages of the electrodes to some desired value. Then, when the test mass moves, the force on it changes with the inverse of the square of the gap, introducing a negative stiffness into the system – a major source of noise. The GRS suspension is design as a current drive. It can be shown that a perfect current drive system does not introduce any such coupling. As the test mass moves, the current drive attempts to keep the charge on the electrode constant by changing the electrode voltage. The result is that the force on the test mass does not change with test mass position – the stiffness is zero. Forces are applied by modulating an AC carrier. The phases of the AC carriers on each electrode are carefully selected to maintain the test mass at a virtual ground, eliminating the need for an injection electrode. The position of the test mass is measured with a series of capacitance bridges using an AC drive signal superimposed on the control signals. The performance of the high precision, low noise GP-B bridge has been measured at 0.1 nm/√Hz above 5 mHz. When the increased gap of the GRS is considered (2 mm vs. 32 μm), the GRS position sensing system should provide 3 nm/√Hz over the measurement band. The front end sensing and forcing electronics are connected to a bank of A/D and D/A converters to translate the analog drive and position signals into their equivalent digital representations for use by the DRS experiment computer. The position of the test mass within the housing is passed to the drag free control software, which commands thrusters to keep the spacecraft centered about the test mass. The same information is used by an electrostatic suspension control law to maintain the orientation of the test mass in the housing, and to provide low frequency control of the secondary test mass in the sensitive direction.

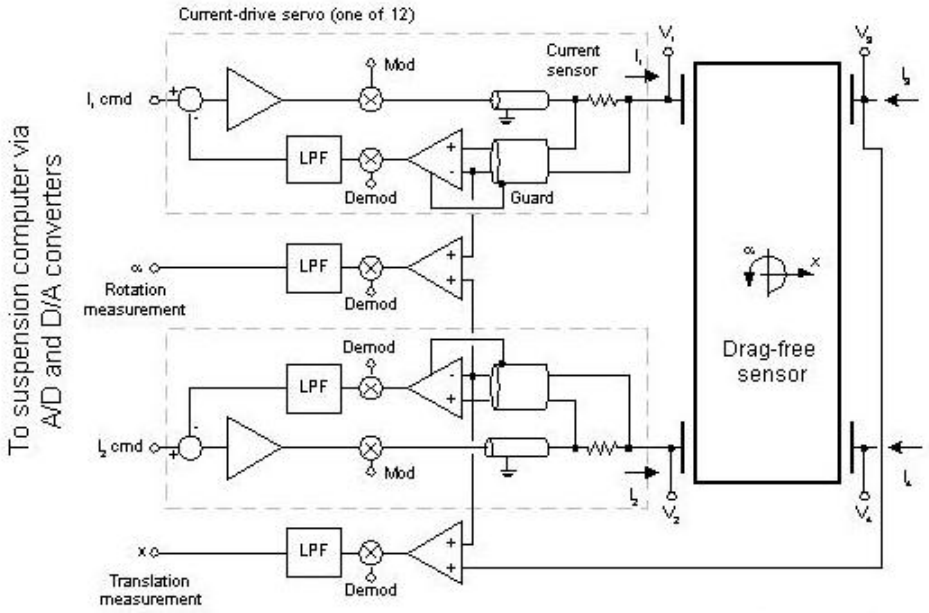


Figure 3: Current Drive Electronics Concept

The housing walls are made from beryllia, a ceramic with thermal conductivity superior to ULE and dimensional stability superior to metals. The six housing plates are positioned precisely and held in place by machined stand-offs in a titanium chassis. Small, spring-loaded stops protrude into the chassis, keeping the test mass from hitting the electrode walls and providing a stable basis for caging the test mass during launch. The test mass is caged during launch to prevent it from damaging the electrode walls or its surface. A single caging plunger pushes the test mass from one corner across the main diagonal and into the stops on the opposing wall. The stops are compressed until they contact the support structure so that the beryllia housing does not carry any of the launch loads. The caging plunger is activated by a pneumatic system, which provides a high pressure, strong caging force for launch and a recaging capability at low pressure and low force on orbit.

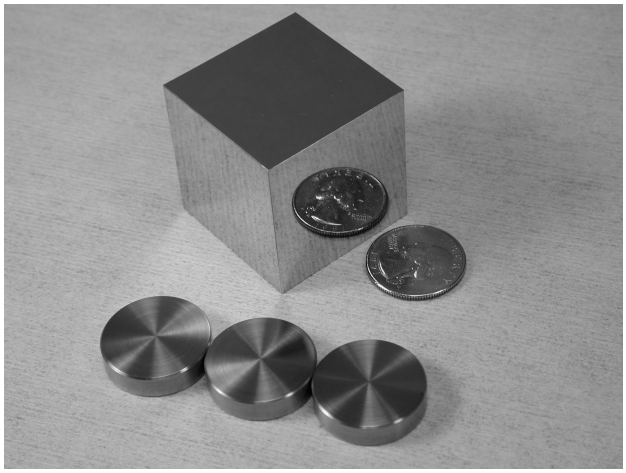

Figure 4: Sample Test Mass and Au/Pt Disks

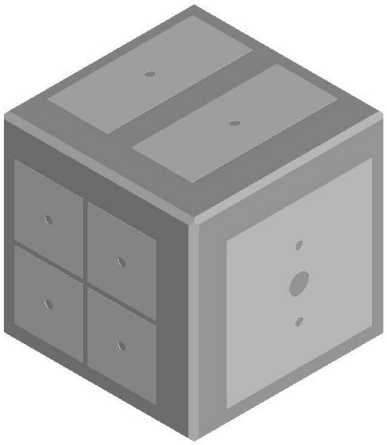

Figure 5: GRS Electrode Layout

During operation the test mass will experience charging rates on the order of $10^{-20}$ C· $s^{-1}$· $g^{-1}$ to $10^{-18}$ C· $s^{-1}$· $g^{-1}$. As the charge increases, coupling to the housing and Lorentz forces increase, degrading the performance of the sensor. The

GRS uses a UV charge control system based on GP-B hardware. This system has a control capability of $10^{-11}$ C and a sensing capability of $5\cdot 10^{-12}$ C. The GP-B system uses a force modulation technique where the position of the test mass is modulated at a frequency high in comparison to the drag free bandwidth. The motion of the position of the test mass is a measure of the potential, and hence, the charge on the test mass. We are studying a different technique developed for GP-B in which the charge of the test mass is measured as a byproduct of the position sensing and forcing operations eliminating the need to force the test mass at high frequency. It may be that this approach is more appropriate for the GRS. Electrons are generated for charge control via UV photoemission. A UV source is connected to the housing via two fibers and the test mass and electrodes are bathed in UV light. By biasing a charge control electrode, the flow of electrons can be made to flow or from the test mass.

## 2. PERFORMANCE ANALYSES

The key performance metric associated with a gravitational reference sensor is the *residual specific force* in the sensitive direction – the x-axis in the case of the GRS. These forces can be divided into two general categories. Direct forces act on the test mass and are independent (to first order) of the motion of the test mass within the housing. In contrast, coupled forces are linearly dependent on the position of the test mass relative to the housing, and hence, to the spacecraft. Coupled forces can modeled as linear springs that couple the accelerations of the test mass to the motion of the spacecraft. It should be noted that the coupled forces act through a coupling tensor so that translation of the test mass in the non-sensitive degrees of freedom will accelerate the test mass in the sensitive direction. The spacecraft position noise is due to noise in the test mass position sensing system, thruster noise and variations in external disturbances (e.g. solar wind). In general, then:

$\vec{f} = \vec{f}_{dir} + [K_{cp}]\vec{x}_{sc}$, where $\vec{f}_{dir}$ are the direct specific forces, $K_{cp}$ is a coupling matrix and $\vec{x}_{sc}$ is the spacecraft position noise.

Analysis of the residual specific forces acting on the test mass and their sources have been carried out by several groups at ESA, NASA and Stanford. One is referred to the work of Keiser[4], Bender, Vitale[5], and Schumaker[6] for further details. Some key results of these analyses are summarized below.

***Direct Residual Specific Forces***

Direct residual specific forces are caused by six major sources: electrostatic forces, magnetostatic forces, thermal gradients across the test mass and housing, fluctuating mass attraction forces, laser power fluctuations, and thermal noise. Further, it has been shown by Vitale and Bender that the time variation of proof mass charge will contribute to the residual specific force noise of the test mass. This source is not described here.

The electrostatic suspension will introduce noise through fluctuations in the electrode voltage and the effect of quantization of the electrode voltage by the digital-to-analog converter. The residual specific force due to the D/A quantization effect has been shown for voltage controlled systems to be:

$$\frac{1}{m}F_{daq} = \frac{1}{m}\frac{2F_p V_{\max}}{V_p 2^N}\sqrt{\frac{1}{12 f_{DA}}},$$ where $F_p$ is the nominal force on the test mass, $V_{max}$ is the maximum electrode voltage, $V_p$ is the preload voltage, $f_{DA}$ is the suspension sample frequency and N are the number of D/A bits. Further work is planned to extend this analysis to the current drive case. However, for the time being, this is seen as an upper bound to the noise. Changes in electrode voltage caused by temperature fluctuations and electronic noise will introduce an acceleration noise. Assuming that the voltage changes on opposite electrodes are independent:

$$\frac{1}{m}F_{elec} = \sqrt{2}\frac{F_p}{m}\frac{\Delta V}{V},$$ where $\Delta V/V$ is the electrode voltage stability in the measurement band.

Variations in the magnetic field at the test mass location will interaction with the test mass in two ways to create residual forces. First, a Lorentz force will be produced by the interaction of the charged proof mass and the fluctuating magnetic field of the sun and solar wind:

$\frac{1}{m} F_{lf} = \frac{Q v_{sc}}{mE} \Delta B$, where Q is the charge on the test mass, $v_{sc}$ is the velocity of the spacecraft, E is the magnetic shielding factor and ΔB is the fluctuation of the magnetic field in the measurement band. Further residual forces are introduced by interactions between the magnetized test mass and the magnetic field produced by the spacecraft:

$\frac{1}{m} \vec{F} = 2 \frac{\chi}{\rho \mu_0} \left\{ \left[ \nabla \vec{B}_0 \right] \vec{b}(t) + \left[ \nabla \vec{b}(t) \right] \vec{B}_0 \right\} + \left[ \nabla \vec{b}(t) \right] \frac{\vec{M}_r}{m}$, where χ and ρ are the magnetic susceptibility and density of the test mass, $B_o$ is the zero frequency magnetic field, b(t) is the time varying magnetic field and $M_r$ is the permanent moment of the test mass.

Temperature gradients across the test mass and the housing will create specific forces through both the radiometer effect and differential radiation pressure on the faces of the test mass. The radiometer effect, caused by differences in the pressure exerted on opposite side of the test mass by a temperature gradient across the housing introduces a residual specific force:

$\frac{1}{m} F_{re} = \frac{1}{m} \frac{AP}{4} \frac{\Delta T}{T}$, where P is the nominal pressure in the housing, A is the area of a test mass side and ΔT/T is the temperature stability of the housing. Similarly, if all surfaces are assumed to be black body radiators, the differential radiation pressure introduced by the same temperature gradient is:

$\frac{1}{m} F_{delr} = \frac{1}{m} \frac{8A\sigma}{3c} T^3 \Delta T$

Note that the factor of 1/3 was introduced by Schumaker to account for the diffuse reflection of radiation from the surface of the test mass.

Similarly, changes in the laser power incident on the surface of the test mass will accelerate the test mass. This can be shown to be:

$\frac{1}{m} F_{las} = \frac{1}{m} \frac{2 n_{ls}}{c}$, where $n_{ls}$ is the laser power fluctuation in the measurement band.

Movement of spacecraft components caused by bulk temperature fluctuations of the spacecraft and material creep will cause the mass attraction forces exerted by the spacecraft on the test mass to change at frequencies in the measurement band. One can consider the motion of a small mass (M) some distance (r) from the test mass. Assuming the test mass can be represented by a point mass, the residual specific force can be shown to be:

$\frac{1}{m} F_{gr} = \frac{2GM}{r^2} \frac{\Delta r}{r}$, where Δr/r is the relative change in position of the disturbing mass.

Damping of the test mass motion will create thermal acceleration noise on the test mass. It has been shown that residual gas damping produces thermal noise proportional to the square root of the housing pressure:

$\frac{1}{m} F_{resg} = 2 \frac{\left( k_B T m_{N2} \right)^{0.25} \left( PA \right)^{0.5}}{m}$, where $m_{N2}$ is the molecular mass of the residual gas and T is the nominal pressure in the housing. Further, Maraner and Vitale[7] have shown that dielectric loss in the capacitance between the electrodes and the test mass cause another acceleration of the test mass:

$$\frac{1}{m}F_{dloss} = \frac{1}{m}2V_p\sqrt{\frac{k_B T\delta_s}{m\omega_{es}C_s}}\left|\frac{\partial C}{\partial z}\right|$$, where δ is the loss tangent of the capacitance, $C_s$ is the stray capacitance and $\omega_{es}$ is the driving frequency of the AC bridge.

***Test Mass Coupling Matrix***

The spring stiffness between the test mass and the housing typically has a negative spring constant, such that motion away from the center of the housing creates forces that tend to exaggerate that motion. This coupling has five sources: electrostatic gradients caused by the presence of the electrostatic suspension and measurement systems, electrostatic gradients caused by work function variations over the surface of the test mass, the interaction between a charged proof mass and the housing, mass attraction gradients caused by the spacecraft, and interactions with the curvature of the magnetic field produced by the spacecraft.

As previously mentioned, the GRS electrostatic suspension system will use an AC current drive system to exert forces on the test mass. If such a system were perfect, changes in test mass location would not affect the force on the test m ass and the coupling term would be zero. Consider the parallel plate equation, written in terms of charge on the plates:

$$F = \frac{Q^2}{2\varepsilon_o A}$$

With a current drive system, the charge on the plates is kept constant as the distance between the plates changes, so the derivative of the force (F) with respect to position (x) is zero. However, implementation effects, such as stray capacitance and the limited bandwidth of the current control system will result in some stray coupling between the electrodes and the test mass. This has been modeled as a voltage controlled suspension in parallel with the current controlled suspension, but exerting only a fraction of the force of a fully voltage controlled suspension (typically, 10%). So, the coupling stiffness is a fraction of the stiffness introduced by a voltage controlled suspension:

$$\frac{1}{m}\frac{\partial F}{\partial x} = \frac{\eta}{m}\frac{\partial}{\partial x}\left(\frac{\varepsilon_o A}{2d^2}V^2\right) = \frac{\eta}{m}\frac{-\varepsilon_o A}{d^3}V^2$$

Local potential variation on the surface of the test mass and electrodes are the source of "patch effects". According to Speake[8], these patches produce stiffness due to both axial motion of the test mass (motion normal to a surface) and due to the shear motion of the test mass (motion parallel to a surface). Further, it is possible for these patches to couple transverse motion of the test mass into accelerations in the sensitive axis. The strength of the coupling constant is proportional to the square of the patch voltage and one over the square of the gap.

The charge on the proof mass will be monitored and controlled by the GRS charge control system, with a maximum acceptable charge of $10^{-10}$ C. This residual charge will couple to image charge created on the electrodes and the ground plane to produce a stiffness between the proof mass and the housing. Using the parallel plate approximation, this stiffness can be shown to be:

$$\frac{1}{m}\frac{\partial F}{\partial x} = -\frac{1}{m}\frac{Q^2}{2d\varepsilon_o A}$$

Gradients in the mass attraction field at the location of the test mass can also be shown to couple motion of the spacecraft into acceleration of the test mass. After careful measurement and control of the spacecraft mass properties, trim masses will be used to offset both the zero frequency mass attraction force and the mass attraction force gradient. If the residual mass is represented by a small mass (M) some distance (r) from the test mass, the coupling term can be shown to be:

$$\frac{1}{m}\frac{\partial F}{\partial x} = -\frac{2GM}{r^3}$$

The final source of coupling between the test mass and the spacecraft are interaction between the test mass and the second derivatives of the magnetic field gradient. In its simplest form, considering a test mass with a remanent moment $M_r$ coaligned with a magnetic field B, the stiffness can be shown to be:

$$\frac{1}{m}\frac{\partial F}{\partial x} = \frac{\partial^2 B}{\partial x^2}\cdot\left(\frac{M_r}{m} + \frac{2\chi}{\rho\mu_o}\right)$$

***The GRS Noise Tree***

The noise sources described above have been collected into a "noise tree", which allows for easy identification of key noise sources and critical design parameters. By varying design and environmental parameters, the noise tree provides a useful tool that aids in the execution of design trade studies. While the tree is too expansive to be shown here, a typical set of cells are shown in Figure 6, below.

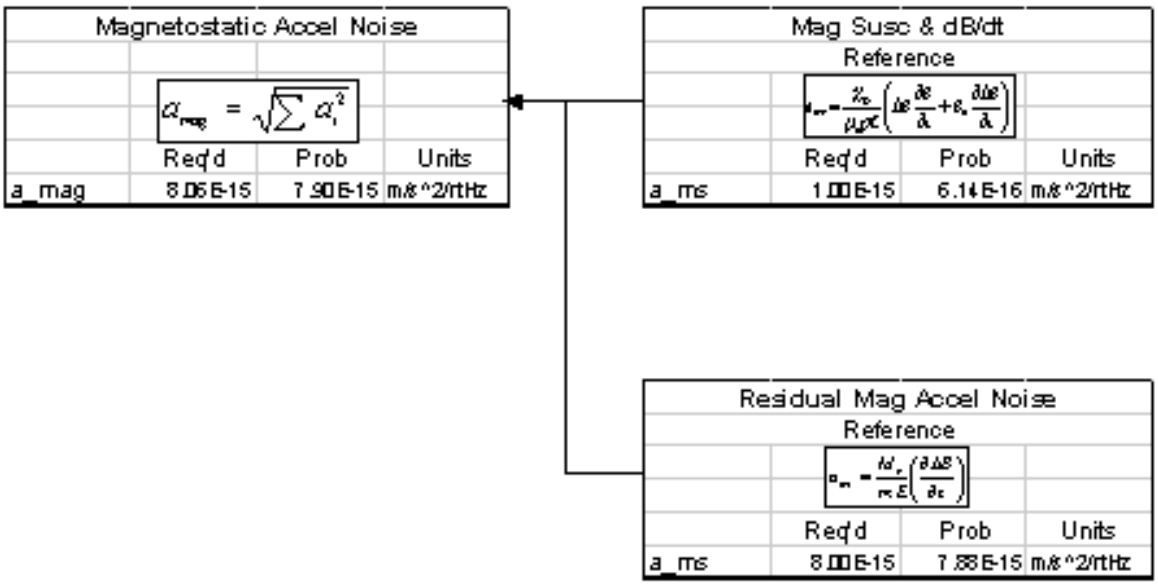


Figure 6: GRS Noise Tree – Direct Magnetic Acceleration Terms

Summaries of the noise analysis terms are shown in Figures 7 and 8, below. As can be seen, the driving direct noise terms are the specific force noise caused by interactions between the magnetized test mass and the changing spacecraft magnetic fields – even when one assumes very tight control of the spacecraft magnetic fields as is the case here. The coupling stiffness of the sensor is dominated by the electrostatic suspension stiffness and the patch effects. Of further concern is the mass attraction force. This can be controlled by careful mapping of the spacecraft mass properties and the addition of trim masses in the vicinity of the GRS.

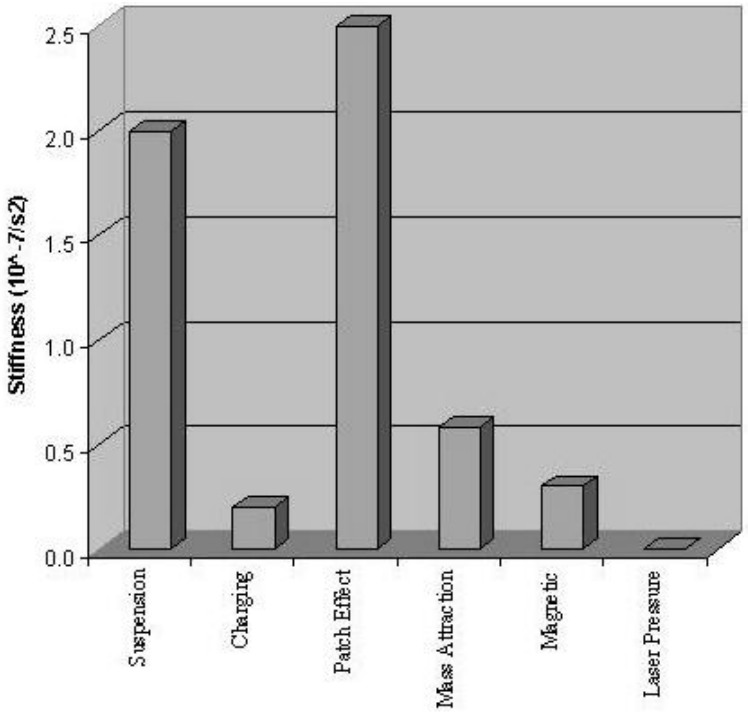


Figure 7: GRS Stiffness Budget

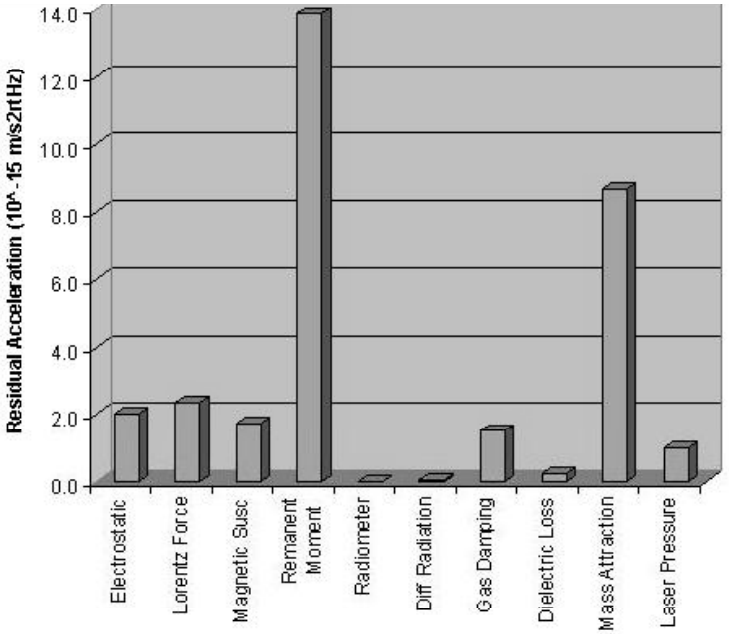


Figure 8: GRS Direct Specific Force Budget

## 4. SUMMARY

When it flies on the SMART-2 spacecraft, the Gravitational Reference Sensor being developed for the New Millennium Program's Disturbance Reduction System will demonstrate an improvement of several orders of magnitude over existing sensors in both residual specific force ($3 \cdot 10^{-14}$ m/($s^2 \cdot \sqrt{Hz}$)) and low frequency coverage (1 mHz to 10 mHz). This is made possible by innovations in the electrostatic suspension electronics, UV charge control system, mechanical design and performance of the related colloid thrusters. A key driving noise source is the remanent moment discovered during routine testing of the Au/Pt alloy. Over the next several months we will be focused on improving our understanding of this remanent magnetization and on ways to reduce both its magnitude and its effect on the per formance of the system.

## 5. ACKOWLEDGEMENTS

This work was performed under JPL contract #1232133 as part of the ST-7 Drag Reduction System, a New Millennium Program.

## 6. REFERENCES

1. Space-Dept, A. P. L. and Guidance Control Laboratory. "A Satellite Freed of all but Gravitational Forces: TRIAD I," *Journal of Spacecraft*. **11**, pp. 637-644, 1974.
2. Hueller, M., et al. "Torsion Pendulum Facility for Ground Testing of Inertial Sensors for LISA," *4th Eduardo Amaldi Conference on Gravitational Waves*, 2001.
3. Wu, C.-H. "DC Electrostatic Gyro Suspension System for the Gravity Probe B Experiment," Stanford University, Stanford, 1993.
4. Keiser, G.M., S. Buchman, W. Bencze, and D. B. Debra, "The Expected Performance of Gravity Probe B Electrically Suspended Gyroscopes as Differential Accelerometers," *Second International LISA Symposium and the Detection and Observation of Gravitational Waves in Space*, 1998.
5. Vitale, Stefano. *System requirements definition for the Lisa Technology Package on board SMART-2*, 2002.
6. Schumaker, Bonny. "Overview of Disturbance Reduction Requirements for LISA," *4th Annual LISA Symposium*, 2002.
7. Maraner, A., S. Vitale, and J.P. Zendri, *Classical and Quantum Gravity*. **13**: p. A129, 1996.
8. Speake, C. C. "Forces and Force Gradients due to Patch Fields and Contact-Potential Differences," *Classical and Quantum Gravity*. **13**, pp. A291-A297, 1996.